Perturbed-angular-correlation measurement of a Fermi to Gamow-Teller mixing ratio in the β decay of ^{19}O

D. M. Perlman and L. Grodzins
Laboratory for Nuclear Science and Department of Physics, M.I.T., Cambridge, Massachusetts 02139

C. E. Thorn
Brookhaven National Laboratory, Upton, New York 11973

(Received 27 February 1978)

Time-differential β-γ angular correlations perturbed by the nuclear quadrupole interaction in a zinc single crystal were used to extract a value of $y = +0.030 \pm 0.015$ for the ratio $C_V M_F / C_A M_{GT}$ of Fermi to Gamow-Teller matrix elements in the allowed β^- decay from the $5/2^+$ ^{19}O ground state to the $5/2^+$, 197 keV state in ^{19}F. This leads to a figure of $M_F = (4.7 \pm 2.4) \times 10^{-3}$ for the isospin-forbidden Fermi matrix element. Other parameters which can be derived from this number are $\alpha = (2.7 \pm 1.4) \times 10^{-3}$ for the admixture of the analog of the ^{19}O ground state in the ^{19}F excited state and $|H_{CD}| = 20 \pm 10$ keV for the effective charge-dependent matrix element. A value of $\omega_0 = +8.5 \pm 0.5$ μsec^{-1} was determined for the nuclear quadrupole interaction of the ^{19}F excited state in a zinc single crystal. The calibration provided by the pure Gamow-Teller decay to the $3/2^+$ 1.554 keV state in ^{19}F was used to remove effects of the implantation process, and data analysis was performed with a model which incorporated the effects of β's backscattered by the thick crystal.

[RADIOACTIVITY ^{19}O; measured β-γ (θ) in Zn single crystal; deduced allowed β decay matrix element, isospin mixing in ^{19}F level, and ω_0 sign for ^{19}F level in Zn.]

I. INTRODUCTION

The application of β-γ time-differential perturbed angular correlations (TDPAC) for measuring the sign of the nuclear quadrupole interaction (NQI) in single crystals has been reported by Raghavan *et al.*[1-3] Following this work, Rots *et al.*[4] utilized β-γ TDPAC to observe a magnetically induced NQI in a ferromagnetic cubic lattice. In this paper we report an experiment which employs β-γ TDPAC to obtain the ratio of Fermi (F) to Gamow-Teller (GT) matrix elements in the allowed β transition from ^{19}O to the first excited state of ^{19}F. This quantity measures the isotopic spin mixing in the nuclear levels involved in the decay.

Isospin mixing is of interest because of the information which it can convey about charge-dependent terms in the nuclear Hamiltonian. Isospin symmetry is broken by the Coulomb force and by the charge dependence of the nuclear force. Allowed β decay is an excellent probe for the existence of isospin mixing in nuclear levels because selection rules restrict the isotopic spin change (ΔT) to 0 in F transitions and to 0 or ±1 in GT transitions. As a consequence, F decay between levels of nominally different isospin can occur only if at least one of the levels contains isospin impurities. In the β^- case the predominant contribution generally is from admixing of the analog of the parent ground state into the level of the daughter nucleus to which β decay proceeds.[5]

In the past, two techniques have been used to measure matrix element ratios in allowed β decay: the angular distribution of β particles from polarized nuclei and the angular correlation of β particles and circularly polarized γ rays. Because of the difficulty of obtaining polarized nuclear sources, most of the available data[6] have been obtained with the latter technique, which suffers from the low efficiency of the polarization measurement. The β-γ TDPAC technique eliminates the need for a polarization measurement.

In the absence of external perturbations, for allowed β decay the β-γ angular distribution is isotropic. For a pure F decay, if the intermediate state is perturbed by the axially symmetric NQI in a single crystal the β-γ correlation remains isotropic. However, under the same perturbation, the correlation for a pure GT decay becomes anisotropic. In the case of a mixed decay, anisotropy whose magnitude depends on the mixing ratio is produced by interference between the two modes of decay.

The magnitude of the observed perturbations also depends on experimental conditions, only some of whose effects can be calculated. Population of nonequivalent sites in the single crystal and radiation damage from the implantation process can alter the perturbation; scattering within the source and geometrical effects must be accounted for. In the

case studied in this experiment, the perturbation amplitude for a pure GT transition leading indirectly to the same intermediate state is simultaneously measured. This allows most of the extraneous effects to be eliminated, and the ratio of matrix elements in the mixed transition can be determined.

In Sec. II, isospin as it relates to β decay is discussed, and the information which can be obtained from a measurement of the matrix element ratio is described. The relevant perturbed angular correlation formalism is given in Sec. III, and the experimental procedure and analysis appear in Secs. IV and V. We conclude with a brief discussion of the results in Sec. VI.

II. ISOSPIN MIXING IN β DECAY

Two matrix elements characterize allowed β decay[5,6]: the Fermi matrix element

$$M_F = \left\langle f \left| \left| \sum_j t_\pm^{(j)} \right| \right| i \right\rangle = \langle f || T_\pm || i \rangle \tag{1}$$

and the Gamow-Teller matrix element

$$M_{GT} = \left\langle f \left| \left| \sum_j t_\pm^{(j)} \vec{\sigma}^{(j)} \right| \right| i \right\rangle . \tag{2}$$

$||i\rangle$ and $\langle f||$ are the initial and final states for the decay, $t_\pm$ are charge raising and lowering operators, and $\vec{\sigma}$ is the spin operator. The sum is taken over all the nucleons. The selection rules for these two modes of decay are summarized in Table I.

Since the Fermi decay operator for β^- decay, T_-, cannot connect states of different isospin, the Fermi matrix element vanishes for decay to states, $T_<$, of lowest isospin ($T = T_3$). Charge-dependent terms in the nuclear Hamiltonian, however, admix into $T_<$ other states of higher isospin which may permit a nonzero Fermi matrix element. The largest such admixture is generally from the analog A of the parent ground state P. For an amplitude α of the analog state admixed in the final state, the Fermi matrix element becomes

$$\begin{aligned} M_F &= \alpha \langle A{:}J^\pi, T, T_3 - 1 || T_- || P{:}J^\pi, T, T_3 \rangle \\ &= \alpha [(T + T_3)(T - T_3 + 1)]^{1/2} \\ &= \alpha \sqrt{2T}, \quad \text{when } T = T_3 . \end{aligned} \tag{3}$$

Treating the charge-dependent terms H_{CD} in the Hamiltonian as a perturbation, the first order expression for the amplitude of the analog state in the final state is

$$\alpha = \frac{\langle T_< || H_{CD} || A \rangle}{\Delta E} , \tag{4}$$

where ΔE is the energy difference between $T_<$ and the analog state.

In β transitions between levels with the same nonzero spin, where both F and GT components may be present, the interference between the two terms is measured by the ratio

$$y = \frac{C_V M_F}{C_A M_{GT}} . \tag{5}$$

C_V and C_A are the weak-interaction vector and axial vector coupling constants. Making use of the comparative half-life, ft, of "superallowed" ($0^+ \rightarrow 0^+$) β decays and the ft value of the decay of interest, the Fermi matrix element can be determined[5]:

$$M_F^2 = \frac{2ft_{\text{superallowed}}}{ft_{\text{decay under study}}} \frac{y^2}{1+y^2} . \tag{6}$$

Nuclear models can be used to calculate H_{CD}, which may be compared with the experimental value of y through Eqs. (3)–(6).

III. PERTURBED CORRELATION

The directional distribution of γ rays from an oriented source [one in which the populations $P(m)$ of the m states of a particular nuclear level are unequal] is sensitive to the alignment, but not to the polarization, of the source. Axially symmetric oriented ensembles of nuclear states are aligned [e.g., $P(m) = P(-m) \neq P(m')$] if they are invariant under reversal of the symmetry axis; these are described in angular correlation formalism[7] by

TABLE I. Selection rules for Fermi and Gamow-Teller matrix elements.

Quantity		Fermi decay	Gamow–Teller decay
Angular momentum	$\Delta J = \lvert J_i - J_f \rvert$	0	0, 1
Parity	$\pi_i \pi_f$	+1	+1
Isotopic spin	$\Delta T = \lvert T_i - T_f \rvert$	0	0, 1

statistical tensors of even rank. Polarized ensembles [e.g., $P(m) \neq P(-m)$] are not symmetric under reversal of the symmetry axis and are described by statistical tensors of odd rank.

Allowed β decay produces either polarization (GT decay) or no orientation (F decay) of the state to which decay proceeds; hence an allowed β-γ directional correlation is isotropic. If, however, following allowed β decay the nucleus in a polarized intermediate state experiences the perturbing effect of an axially symmetric NQI whose symmetry axis is not collinear with the axis of polarization (e.g. the interaction between the nuclear quadrupole moment and the axially symmetric electric field gradient in a noncubic single crystal), the nuclear spin precesses about the symmetry axis of the interaction. Nuclei in $+m$ and $-m$ states precess in opposite directions, causing the initial polarization to be converted into a time-varying alignment which appears as an oscillatory anisotropy in the emission pattern of the deexciting γ rays. In a time-differential angular correlation, terms appear containing factors of the form $\sin n\omega_0 t$, where n is an integer and ω_0 is the fundamental quadrupole frequency.[3] The experimentally observed sign and frequency of ω_0 yield the sign and magnitude of the NQI, while the amplitude of the terms is a function of the mixing ratio y. Thus it is possible to extract mixing ratios (and hence the charge-dependent matrix element $\langle \| H_{CD} \| \rangle$) by β-γ TDPAC experiments.

The β-γ perturbed angular correlation in a coordinate system with the z axis parallel to the symmetry axis of the perturbation (in these experiments the crystal c axis) is given by the expression[1]

$$W(\vec{k}_1, \vec{k}_2, t) = \sum_{k_1 k_2} \sum_{N_1 N_2} \frac{(-1)^{k_1 + k_2} A^{\beta}_{k_1} Q^{\beta}_{k_1} A^{\gamma}_{k_2} Q^{\gamma}_{k_2}}{[(2k_1+1)(2k_2+1)]^{1/2}} \times G^{N_1 N_2}_{k_1 k_2}(t) Y^{*}_{k_1 N_1}(\theta_\beta \phi_\beta) Y_{k_2 N_2}(\theta_\gamma \phi_\gamma) , \tag{7}$$

where A^{β}_{k} are particle parameters describing the β decay, A^{γ}_{k} are γ-ray angular correlation coefficients, Q_k are attenuation factors which account for the finite solid angles of the two detectors, $G(t)$ are perturbation coefficients containing the effect of extranuclear perturbations, and the Y_{kN} are spherical harmonics. θ_β, ϕ_β and $\theta_\gamma, \phi_\gamma$ are polar and azimuthal angles for the β and γ emission directions. For allowed β decay between levels I_β and I, the particle parameters have the form

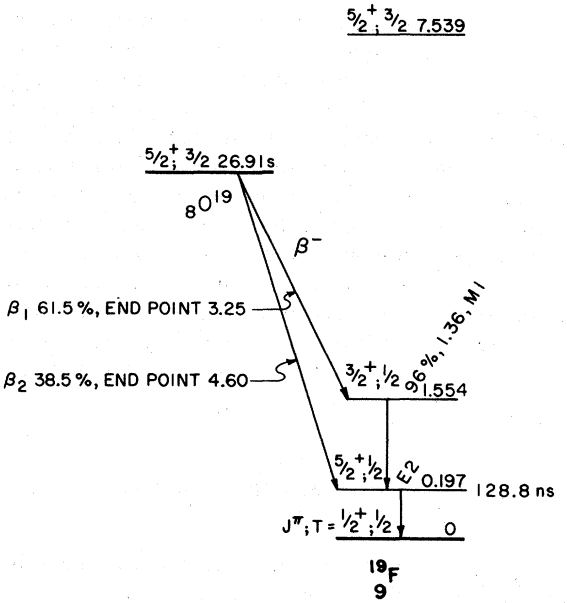

FIG. 1. Decay scheme for $^{19}O \rightarrow {}^{19}F$. Spin-parity and isospin assignments are shown. The level in ^{19}F at 7.539 MeV is the analog of the ^{19}O ground state.

$$A^{\beta}_0 = 1; \quad A^{\beta}_1 = \frac{2}{3}\frac{p}{E}\frac{yF_1(01 I_\beta I) \pm F_1(11 I_\beta I)}{1+y^2} , \tag{8}$$

where y is the matrix element ratio [Eq. (5)], p and E are the momentum and energy of the β, and F_1 is defined in Ref. 8. The plus and minus signs refer to negaton and positon decay, respectively. The functional forms and properties of the other factors in Eq. (7) have been discussed in the literature (see, e.g., Ref. 3 for a review).

The expression for the correlation [Eq. (7)] must be evaluated for each of the two β^- decays leading from the ^{19}O ground state to the $\frac{5}{2}^+$ state in ^{19}F (Fig. 1).

The pure GT transition with 3.25 MeV endpoint energy, β_1, leads to the 1.554 MeV $\frac{3}{2}^+$ state of ^{19}F, which populates the 197 keV $\frac{5}{2}^+$ state via a 1.36 MeV γ ray. The decay with an endpoint of 4.60 MeV, β_2, feeds the 197 keV state directly and on the basis of angular momentum and parity may contain both F and GT components, but F decay is forbidden by isospin selection rules. Inserting the form for $G(t)$ which describes an axially symmetric NQI in a single crystal[9] and performing the summations, the angular correlation for each β can be written

$$W(\vec{k}_\beta, \vec{k}_\gamma, t) = 1 + 2\sqrt{105}\, \tilde{A}^{\beta}_1 Q^{\beta}_1 \sin\theta_\beta \sin\theta_\gamma \cos\theta_\gamma \sin(\phi_\gamma - \phi_\beta) \times \{ [\tfrac{4}{245} Q^{\gamma}_2 - \tfrac{2}{147} Q^{\gamma}_4 (7\cos^2\theta_\gamma - 3)] \sin\omega_0 t + [\tfrac{1}{49} Q^{\gamma}_2 + \tfrac{1}{147} Q^{\gamma}_4 (7\cos^2\theta_\gamma - 3)] \sin 2\omega_0 t \} , \tag{9}$$

where $\tilde{A}_1^\beta$ is the appropriate particle parameter (including the effects of any unseen γ). The amplitudes of the two time-dependent terms in this expression as a function of the γ emission angle θ_γ, with $(\phi_\gamma - \phi_\beta) = \theta_\beta = 90°$, are illustrated for the case of point detectors in Fig. 2. At $\theta_\gamma \cong 40°$ with point detectors the $\sin\omega_0 t$ term vanishes and the correlation assumes the simple form

$$W(t) = 1 + 0.28\tilde{A}_1^\beta \sin 2\omega_0 t . \tag{10}$$

Reversing the β direction or changing θ_γ to $\pi - \theta_\gamma$ changes the sign of the perturbation, as is evident from Eq. (9). These geometrical symmetries can be used to confirm that the perturbation is due to the NQI.

The particle parameter for the β_1 branch must be modified to include the effect of the unobserved 1.36 MeV γ ray, which is predominantly $M1$ in character.[10] This is accomplished by multiplying $A_{k_1}^\beta$ by an additional coefficient

$$U_{k_1}(I_a I_b) = \sum_{L_2} (-1)^{k_1 + L_2} \begin{Bmatrix} I_b & I_b & k_1 \\ I_a & I_a & L_2 \end{Bmatrix} \times \langle I_b \| L_2 \pi_2 \| I_a \rangle^2 , \tag{11}$$

where I_a and I_b are the spins of the two levels involved in the unseen γ transition and L_2 and π_2 are the multipolarity and parity of the γ. This expression includes a factor of $(-1)^{k_1}$ which is missing from the standard definition[8] and is of significance when the intermediate state is produced in a polarized condition, requiring terms of odd k_1 in Eq. (7).

For β energies below 3.25 MeV, the perturbed correlation displays a strong energy dependence, reflecting the changing ratio of β particles present from the two branches. This dependence can be displayed by summing the correlations for both β particles, which is formally equivalent to substituting in Eq. (9) the effective particle parameter

$$\tilde{A}_1^\beta(E) = f_{\beta_1}(E) A_1^{\beta_1} U_1(\tfrac{3}{2}, \tfrac{5}{2}) + f_{\beta_2}(E) A_1^{\beta_2} \tag{12}$$

with $f_{\beta_1}(E)$ = fraction of decays to the $\frac{3}{2}^+$ state at a β energy E, and $f_{\beta_2}(E)$ = fraction of decays to the $\frac{5}{2}^+$ state. The resulting dependence of the amplitude of this total correlation on the β energy is shown in Fig. 3 for various values of the mixing ratio y. The amplitude of the correlation at highest β energies is most sensitive to the mixing ratio; the lowest energy β particles, which are dominated by the pure GT transition to the $\frac{3}{2}^+$ ^{19}F state, serve to normalize the correlation, removing effects such as those due to detector geometry and the implantation process, leaving only the dependence on the mixing ratio.

IV. EXPERIMENT

The sign and magnitude of the NQI for the 197 keV state of ^{19}F in Zn single crystals has been measured previously with Coulomb excitation

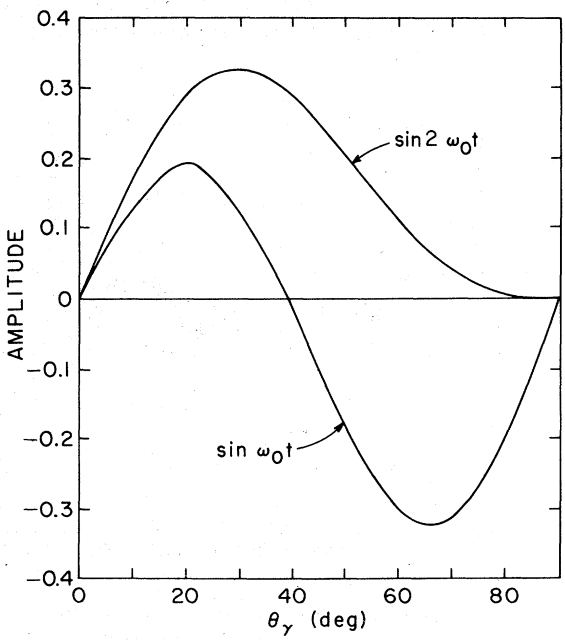

FIG. 2. Dependence on γ emission angle of coefficients of the $\sin\omega_0 t$ and $\sin 2\omega_0 t$ terms in Eq. (9) with solid angle factors and particle parameter set to 1.

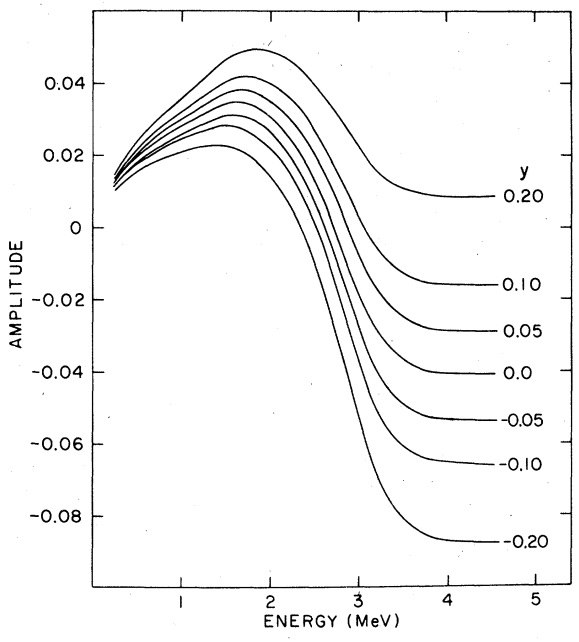

FIG. 3. Calculated amplitudes of the time-dependent correlation [Eq. (9)] for a set of values of the mixing ratio y. These curves, computed for the β_{up}-γ_2 geometry in Fig. 4, include the effects of corrections discussed in Sec. V.

TDPAC methods.[11,12] These data, which could be used to confirm the β-γ TDPAC observations, led us to adopt the same crystals for these measurements.

A 35 MeV ^{18}O beam from the BNL MP6 tandem van de Graaff accelerator incident on a thin beryllium foil produced the 26.91 sec ^{19}O activity[13] by the ^{9}Be(^{18}O,^{19}O)^{8}Be reaction. The ^{19}O reaction product emerging from the back of the target implanted itself in a 1 cm diam, 1 mm thick zinc single crystal mounted at 45° to the beam direction on a Delrin block (rabbit) which was shuttled to a counting site after activation. Narrow collimation of the ^{19}O and continuous monitoring of the rabbit location during irradiation insured that all activity was restricted to the crystal surface. X-ray diffraction pictures taken prior to and following the experiment established the absence of radiation and mechanical damage to the crystal in the course of the measurement. Irradiation and counting were alternated within a 65-sec period.

At the counting site at a distance of 2 cm from the crystal center, a 5.1 cm diam by 3.8 cm thick plastic scintillator mounted on a fast photomultiplier tube detected β particles either above or below the plane formed by the crystal c axis and the γ detector axes. Two 7.6 cm × 7.6 cm integral line NaI(Tl) γ detectors were located 7.25 cm from the crystal at angles of $\theta = 40°$ and 140° (see Fig. 4). This choice of detector positions enabled us to observe the sign changes in the perturbation predicted by theory (Sec. III), confirming unequivocally the presence of an axially symmetric NQI. Standard fast-slow coincidence electronics were employed to store individual β-γ (197 keV) time spectra for a series of β energies ranging from 0 to 4.6 MeV. Coincidences with each of the two γ detectors were stored separately, and runs were made alternately with the β detector above and below the plane of the γ detectors.

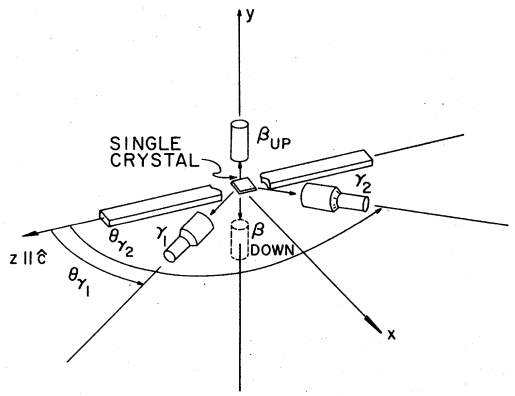

FIG. 4. Detector-crystal geometry used in β-γ TDPAC measurements.

V. ANALYSIS

β-γ time spectra were analyzed independently for the two γ detectors by subtracting constant backgrounds (due to random events), normalizing runs with β direction up to those with β direction down, and forming the ratio

$$\frac{W(\text{up}) - W(\text{down})}{W(\text{up}) + W(\text{down})}$$

for each β energy bin to eliminate the exponential decay. Frequencies of the time-varying perturbation were extracted from each ratio spectrum by a least squares fitting program. Owing to the smaller amplitude of the $\sin\omega_0 t$ term (25% of that for the $\sin 2\omega_0 t$ term with our choice of detector positions and solid angles) and limitations of our statistics, only the higher frequency component could be identified in the data. The frequency was fixed at a weighted average of the fit values, and the amplitude of the perturbation was obtained for each β energy bin by re-fitting the ratio spectra. Typical data (for a central β energy of 1.45 MeV) are shown in Fig. 5. These clearly demonstrate the reversal in sign of the perturbation with γ detector angle that is predicted by theory. A value of $\omega_0 = +8.5 \pm 0.5\ \mu\text{sec}^{-1}$ was obtained for the quadrupole frequency, in excellent agreement with $+7.9 \pm 1.0$ and $+8.73\ \mu\text{sec}^{-1}$ from Coulomb excitation work.[11,12]

The energy calibration for the β detector was obtained using Compton spectra of γ rays with energies up to 4.43 MeV. These spectra were fitted to the Klein-Nishina formula folded with a Gaussian resolution function whose width was allowed to vary

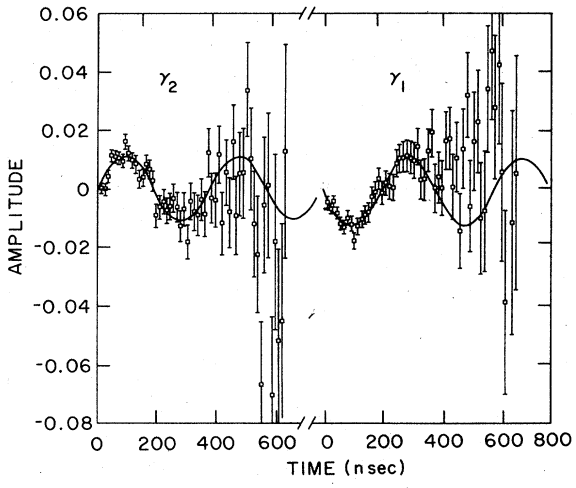

FIG. 5. Time dependence of ratio spectra $[W(\text{up}) - W(\text{down})]/[W(\text{up}) + W(\text{down})]$ at a central β energy of 1.45 MeV, displaying reversal in sign of the nuclear quadrupole perturbation for γ emission angles $\theta_{\gamma_1} = 40°$ (right) and $\theta_{\gamma_2} = 140°$ (left). See Fig. 4.

as the square root of its center energy.[14]

The analysis to extract the mixing ratio y from experimentally determined energy-dependent perturbation amplitudes was performed in two parts. First, the relative contributions of the ^{19}O decay components which appear in the time spectra were determined by careful analysis of the β detector spectrum. Second, these components were used to generate theoretical curves for the perturbation amplitude as a function of energy and y which were then fitted to the experimental perturbation amplitudes.

Specifically, in the first step of the analysis, a best fit was generated to the energy spectrum of events in the β detector in coincidence with a 197 keV γ ray in one γ detector by summing the spectra of five types of events: β particles from each of the two ^{19}O decay groups directly entering the detector, β particles from these groups which have been backscattered by the crystal, and the electrons due to 1.37 MeV γ rays Compton scattered in the plastic scintillator. The spectra of the unscattered β particles were derived from the branching ratio and end point energies cited by Alburger *et al.*[15] The Klein-Nishina formula was employed to reproduce the Compton spectrum.

A simple model was adopted to calculate the spectra of β particles backscattered by the saturation thickness zinc crystal. The backscatter energy distribution for monoenergetic electrons incident on a scattering surface depends rather weakly on the primary energy and more strongly on the angles of incidence and observation. A universal curve[16] (taken with electrons incident on a thick Cu target) representing an average scattering geometry and energy for our experiment was used, and backscatter energy distributions were generated by folding the curve separately with the spectra for the two unscattered β groups. In this process, the total backscatter probability was taken to be independent of the primary energy. To estimate the systematic error which might be introduced by this method, a second curve with significantly different shape,[17] representing a much smaller β scattering angle, was also tried. The two curves are shown in Fig. 6, marked A and B, respectively.

The energy distributions for scattered and unscattered β particles and Compton events subsequently were folded with the detector response function and a fit was made to the experimental spectrum. Provision was made for energy loss by β particles in the 60 mg/cm^2 detector covering and for β-γ summing (which was negligible). The ratio of high to low energy end point β particles was fixed at the branching ratio[15] for scattered as well as unscattered spectra. Only the overall percentage of backscattered β particles (backscatter fraction) and the Compton efficiency of the detector (defined here as a fraction of the number of unscattered 3.25 MeV end point β particles) were allowed to vary. Our ability to reproduce the data using curve A (Fig. 6) for the backscatter distribution is illustrated in Fig. 7. Also shown are the individual components which comprise the spectrum prior to folding with the detector response function. We obtain $(51.3 \pm 2.5)\%$ for the backscatter fraction and $(14.1 \pm 2.2)\%$ for the Compton efficiency. The fit achieved with curve B was poorer. The stated uncertainties include estimates of possible systematic errors introduced by the choice of shape for the backscatter energy distribution and by uncertainties in the β detector window thickness. Our value for the backscatter fraction corresponds well with a figure of approximately 45% for the same backscatter geometry measured with a ^{32}P source on a thick copper backing.[18]

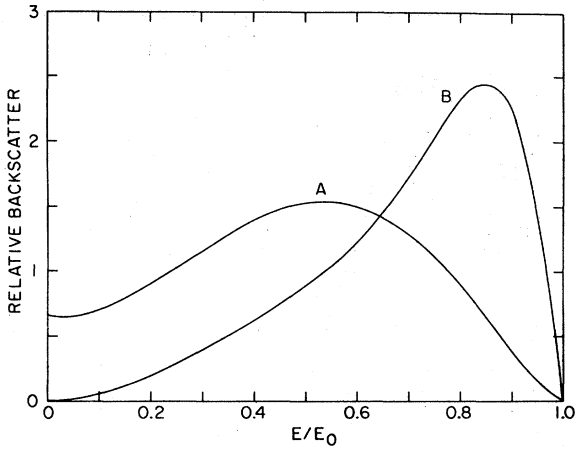

FIG. 6. Energy distributions for monoenergetic electrons backscattered from a saturation thickness scatterer. The two curves shown correspond to different scattering geometries, as discussed in the text.

In the second step in the analysis, each of the component spectra was multiplied by its appropriate correlation and the results were summed to produce curves for the energy-dependent perturbation amplitudes. Correlations for unscattered β particles were calculated from Eq. (9) utilizing formulas in Ref. 19 to compute solid angle correction factors for the β detector and tables in the same reference to determine those for the γ detectors.

It was assumed that backscattered particles seen by the β detector originated with equal probability from all directions entering the crystal surface (so-called diffuse backscattering[18]). The correlations for backscattered β particles were then cal-

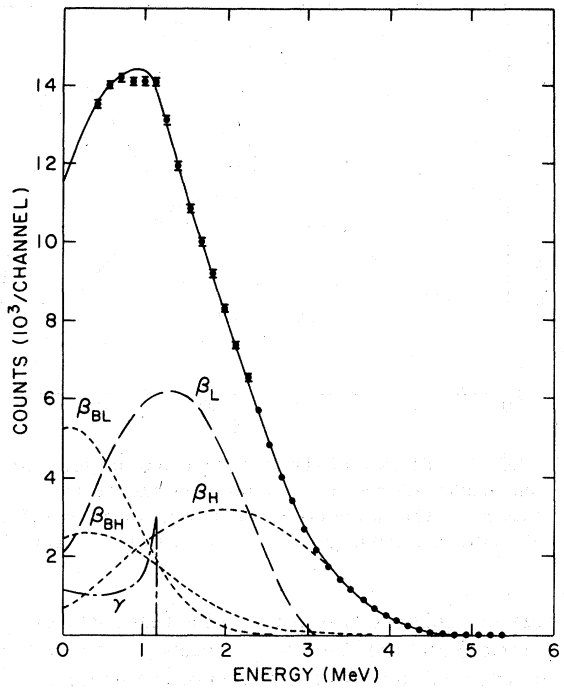

FIG. 7. Experimental energy spectrum of events in β detector coincident with a 197 keV γ ray. Best fit is shown by a solid line. Components of the fit also shown are unscattered β particles (β_L and β_H), backscattered β particles (β_{BL} and β_{BH}), and the Compton spectrum of 1.37 MeV γ rays (γ). Finite resolution of the β detector is not included in the component spectra.

culated separately for the two branches by integrating Eq. (9) over all β emission angles pointing into the crystal. Formally, this is equivalent to deriving the correction factors for a detector subtending the same solid angle. The explicit forms of these correlations are listed in Table II. It should be noted that for all values of y less than 0.169, the perturbation for the 4.60 MeV end point group is opposite in sign to that for the 3.25 MeV end point group. It can also be seen that the perturbation for backscattered β particles differs in sign from that for unscattered β particles from the same group, since the crystal normal in the direction of the surface occupies the opposite hemisphere from the one defined by the β detector direction, reversing the sign of the angle $\Phi_\gamma - \Phi_\beta$.

All of the β-γ correlations display change in the sign of the perturbation with reversal of the β direction; each contributes time-varying terms to the ratio spectra discussed earlier in this section. In contrast, the 1.37 MeV–197 keV γ-γ correlation is unaffected by change of direction of the first radiation. It therefore attenuates the amplitude of the perturbation observed in the ratio spectrum for energies below the Compton edge for the 1.37 MeV γ-ray.

A χ^2 search yielded the best fit (χ^2 per degree of freedom = 1.58) displayed in Fig. 8, for a value of $y = +0.030 \pm 0.015$. The error quoted here is one standard deviation ($\pm 1\sigma$). A plot of χ^2 vs y appears in Fig. 9. The value of y obtained using the alternative backscatter distribution, curve *B*, was $+0.036 \pm 0.016$ (with $\chi^2/\nu = 1.39$). From the overall

TABLE II. β-γ correlations used in ^{19}O–^{19}F β-γ TDPAC experiment. β appeared in coincidence with a 197 keV γ ray in ^{19}F. Solid angle correction factors are calculated for detector geometry discussed in text.

β group	Perturbed correlation
3.25 MeV end point; unscattered	$1+ (p/E)\sin\theta_\beta \sin\theta_\gamma \cos\theta_\gamma \sin(\phi_\gamma - \phi_\beta)$ $\times\{[0.110 - 0.0611(7\cos^2\theta_\gamma - 3)]\sin\omega_0 t$ $+[0.137 + 0.0305(7\cos^2\theta_\gamma - 3)]\sin 2\omega_0 t\}$
4.60 MeV end point; unscattered	$1 - \frac{p}{E}\frac{0.1952 - 1.155y}{1+y^2}\sin\theta_\beta \sin\theta_\gamma \cos\theta_\gamma \sin(\phi_\gamma - \phi_\beta)$ $\times\{[0.268 - 0.149(7\cos^2\theta_\gamma - 3)]\sin\omega_0 t$ $+[0.335 + 0.0745(7\cos^2\theta_\gamma - 3)]\sin 2\omega_0 t\}$
3.25 MeV end point; backscattered[a]	$1+ (p/E)\sin\theta_N \sin\theta_\gamma \cos\theta_\gamma \sin(\phi_\gamma - \phi_N)$ $\times\{[0.0589 - 0.0327(7\cos^2\theta_\gamma - 3)]\sin\omega_0 t$ $+[0.0734 + 0.0163(7\cos^2\theta_\gamma - 3)]\sin 2\omega_0 t\}$
4.60 MeV end point; backscattered[a]	$1 - \frac{p}{E}\frac{0.1952 - 1.155y}{1+y^2}\sin\theta_N \sin\theta_\gamma \cos\theta_\gamma \sin(\phi_\gamma - \phi_N)$ $\times\{[0.144 - 0.0798(7\cos^2\theta_\gamma - 3)]\sin\omega_0 t$ $+[0.180 + 0.0399(7\cos^2\theta_\gamma - 3)]\sin 2\omega_0 t\}$

[a] p and E are the momentum and energy of the β prior to undergoing backscattering. θ_N and ϕ_N are the polar and azimuthal angles of the crystal normal pointing into the surface.

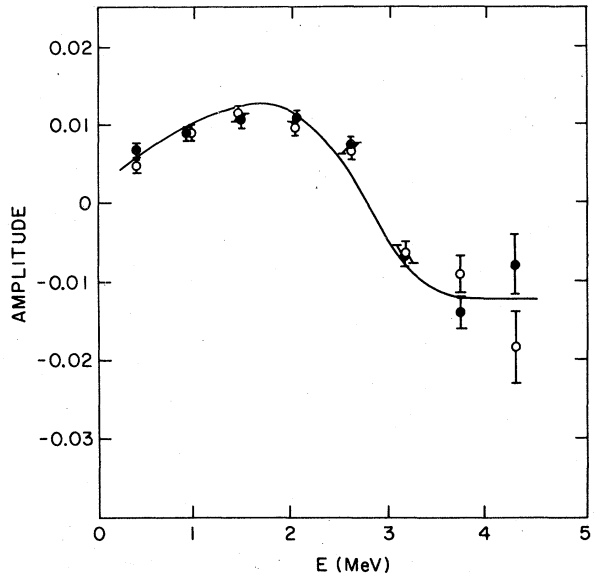

FIG. 8. Amplitudes of the time-dependent perturbation measured with γ detectors 1 (open circles) and 2 (closed circles) as a function of β energy. Solid line is the best fit (for $y = +0.030$). For illustrative purposes the sign of the detector 1 amplitude has been reversed.

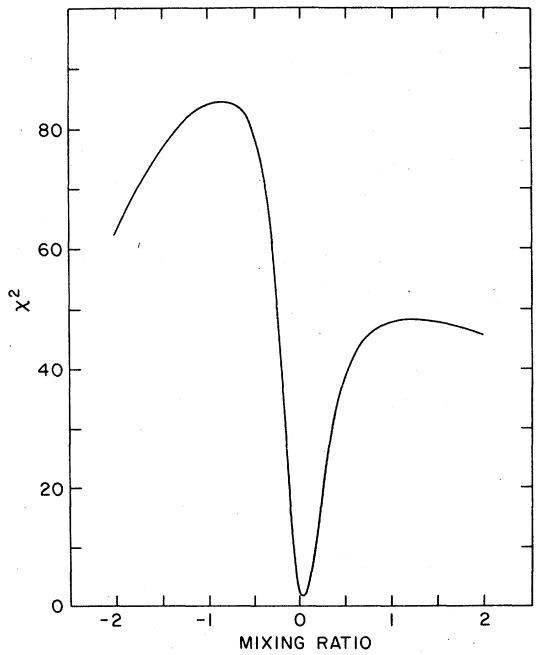

FIG. 9. χ^2 for the fit to the experimental perturbation amplitudes shown in Fig. 8 as a function of the mixing ratio y.

normalization, it can be determined that the number of nuclei stopping on sites where they experience the full axially symmetric NQI is approximately 35%. This figure may be compared with a figure of 45% from the Coulomb excitation work.[11] The smaller value could result from the effects of recoil of the implanted nuclei caused by emission of the β.

A summary of the quantities defined in Sec. II which can be derived from the mixing ratio appears in Table III. The values $ft_{\text{superallowed}} = 3088.6 \pm 2.1$ (Ref. 20) and $\log ft = 5.4$ (Ref. 15) for the mixed decay were adopted for these calculations. The location of the analog of the ^{19}O ground state at 7.539 MeV in ^{19}F was taken from Ref. 21. Reference 6 contains a compilation of all experimentally measured values of the isospin impurity α deduced from β decay experiments. Our measurement is consistent with those for other nuclei in this mass region.

IV. DISCUSSION

In our analysis we have ignored possible energy-dependent effects which could be produced by nuclear recoil from the β and/or (in the case of the lower end point branch) subsequent γ decay. The energy imparted to the nucleus in these processes often is sufficient to overcome its binding energy in the lattice (approximately 30 keV). The figure we find for nuclei occupying good sites is slightly lower than that observed in Coulomb excitation experiments[11] (which directly populate the 197 keV ^{19}F state during the implantation process) and may, in fact, be evidence for the presence of recoil effects. However, our model does provide a detailed fit to the data without recourse to additional corrections.

A number of theoretical calculations have been made of isospin impurities in nuclear levels populated by allowed β decay (see Ref. 6 for an extensive review). These generally incorporate shell or collective model wave functions and introduce isospin mixing through the Coulomb interaction. In some cases an empirical charge-dependent non-Coulomb potential has been added. Bertsch and Wildenthal[22] and Yap[23-25] have investigated isospin mixing in the s-d shell nuclei ^{20}Ne and ^{24}Mg; their

TABLE III. Quantities derived from measurement of mixing ratio for $^{19}\text{O}(\frac{5}{2}^+) \rightarrow {}^{19}\text{F}(\frac{5}{2}^+)$ β decay.

y	$M_F \times 10^3$	$\alpha \times 10^3$	$\lvert H_{CD} \rvert$ (keV)
0.030 ± 0.015	4.7 ± 2.4	2.7 ± 1.4	20 ± 10

calculations give order-of-magnitude agreement with experimental results, but the predictions are very sensitive to the wave functions chosen. For the most part, they are unable to separate Coulomb from non-Coulomb contributions to isospin breaking. Kahana[26] finds it necessary to introduce a short-range, charge-dependent interaction in a shell model calculation in order to reproduce Coulomb energy shifts in the $A = 18$ region. The magnitude of the non-Coulomb charge-dependent potential usually is estimated to be a few percent,[5,27] although we are unaware of any computations which have been made of isospin mixing in ^{19}F.

This nucleus is particularly attractive theoretically because in a simple shell model calculation, with only one proton outside the closed core, the Coulomb force among the valence nucleons vanishes, thus magnifying charge dependent effects among these nucleons.

The β-γ TDPAC technique outlined here provides a valuable complement to the limited number of methods available for investigating isospin impurities in nuclear levels and, in conjunction with accurate shell model calculations, such measurements should add considerably to our understanding of the charge dependence of the nuclear interaction.

ACKNOWLEDGMENTS

We would like to thank Dr. Otto Klepper, who clarified the formalism used in calculating the angular correlations. Dr. Stephen Steadman provided invaluable assistance in the course of the experiment and has been the source of many constructive suggestions. One of us (C. E. T.) would like to acknowledge useful discussions with Dr. D. J. Millener. We also wish to thank the staff of the Brookhaven National Laboratory tandem Van de Graaff, who aided in the construction of apparatus and in running experiments. This work was supported in part through funds provided by the U. S. Energy Research and Development Administration under Contract No. EY-76-C-02-3069. *000.

[1]R. S. Raghavan, P. Raghavan, and E. N. Kaufmann, Phys. Rev. Lett. 31, 111, 802(E) (1973).
[2]P. Raghavan, R. S. Raghavan, and E. N. Kaufmann, Phys. Lett. 48A, 131 (1974).
[3]R. S. Raghavan, P. Raghavan, and E. N. Kaufmann, Phys. Rev. C 12, 2022 (1975).
[4]M. Rots, F. Namavar, and R. Coussement, Phys. Rev. Lett. 34, 1099 (1975).
[5]R. J. Blin-Stoyle, *Fundamental Interactions and the Nucleus* (North-Holland, Amsterdam, 1973).
[6]S. Raman, T. A. Walkiewicz, and H. Behrens, At. Data Nucl. Data Tables, 16, 451 (1975).
[7]R. M. Steffen and K. Alder, in *The Electromagnetic Interaction in Nuclear Spectroscopy*, edited by W. D. Hamilton (North-Holland, Amsterdam, 1975).
[8]H. Frauenfelder and R. M. Steffen, in *Alpha-, Beta-, and Gamma-Ray Spectroscopy*, edited by K. Siegbahn (North-Holland, Amsterdam, 1965).
[9]L. Grodzins and O. Klepper, Phys. Rev. C 3, 1019 (1971).
[10]A. R. Poletti, J. A. Becker, and R. E. McDonald, Phys. Rev. 182, 1054 (1969).
[11]R. Brenn, G. D. Sprouse, G. Yue, and O. Klepper, Nucl. Phys. A265, 35 (1976).
[12]O. Klepper and B. Hoyler (unpublished).
[13]N. B. Gove and M. J. Martin, Nucl. Data Tables A10, 205 (1971).
[14]R. Van Lieshout, A. H. Wapstra, R. A. Ricci, and R. K. Girgis, in *Alpha-, Beta-, and Gamma-Ray Spectroscopy* (see Ref. 8).
[15]D. E. Alburger, A. Gallmann, and D. H. Wilkinson, Phys. Rev. 116, 939 (1959).
[16]H. Frank, Z. Naturforsch. 14a, 247 (1959).
[17]W. Bothe, Z. Naturforsch. 4a, 542 (1949).
[18]H. H. Seliger, Phys. Rev. 88, 408 (1952).
[19]M. J. L. Yates, in *Alpha-, Beta-, and Gamma-Ray Spectroscopy* (see Ref. 8).
[20]S. K. Bhattacherjee, S. K. Mitra, and H. C. Padhi, Nucl. Phys. A96, 81 (1967).
[21]J. H. Aitken, A. E. Litherland, W. R. Dixon, and R. S. Storey, Phys. Lett. 30B, 473 (1969).
[22]G. F. Bertsch and B. H. Wildenthal, Phys. Rev. C 8, 1023 (1973).
[23]C. T. Yap, Nucl. Phys. A100, 619 (1967).
[24]C. T. Yap, Nucl. Phys. A142, 161 (1970).
[25]C. T. Yap and C. S. Tee, Nucl. Phys. A165, 497 (1971).
[26]S. Kahana, Phys. Rev. C 5, 63 (1972).
[27]E. M. Henley, in *Isospin in Nuclear Physics*, edited by D. H. Wilkinson (North-Holland, Amsterdam, 1969).